



On the Stability of LiFePO₄ Olivine Cathodes under Various Conditions (Electrolyte Solutions, Temperatures)

Maxim Koltypin,^a Doron Aurbach,^{a,*} Linda Nazar,^b and Brian Ellis^b

^aDepartment of Chemistry, Bar-Ilan University, Ramat-Gan 52900, Israel

^bUniversity of Waterloo, Waterloo, Ontario, Canada

LiFePO₄ is one of the most important cathode materials for Li-ion batteries studied over the past few years. Impressive work has revealed important structural aspects and the correlations between structure and composition and electrochemical properties. Fewer efforts have been devoted to the surface chemical aspects of this material. We report herein on a study of the stability aspects of LiFePO₄ at two temperatures, 30 and 60°C. Three types of solutions were used based on EC-DMC 1:1 solvent mixtures those involving no acidic contamination (using LiClO₄ as the electrolyte), those contaminated by HF (using LiPF₆ as the Li salt), and LiPF₆ solutions deliberately contaminated with H₂O. Iron dissolution from LiFePO₄ in these electrolytes, as well as the electrochemical response as a function of solution composition and aging, were studied at the two temperatures. The effect of additives that neutralize acidic species in solution was also studied. In general, LiFePO₄ develops a unique surface chemistry. Highly stable behavior of LiFePO₄ cathodes, without any substantial iron dissolution at elevated temperatures, was observed and measured when the solution contains no acidic or protic contaminants.
© 2006 The Electrochemical Society. [DOI: 10.1149/1.2403974] All rights reserved.

Manuscript submitted September 14, 2006; revised manuscript received November 9, 2006.
Available electronically December 18, 2006.

LiFePO₄ olivine is one of the most important cathode materials for Li-ion batteries studied in recent years. Olivine compounds are promising candidates for replacing standard LiCoO₂ cathodes that are currently used in commercial Li-ion batteries because of the high reversibility of their lithiation process, their relative low cost as compared to most other relevant cathode materials for Li-ion batteries, and because of their environmental friendliness.¹ LiFePO₄ has a theoretical capacity of 170 mAh/g and a redox potential around 3.5 V vs Li/Li⁺.² This provides an energy density comparable to compounds such as LiCoO₂,³ LiNiO₂,³ and LiMn₂O₄.³ Although compounds such as LiCoO₂ have higher theoretical capacities, the full intercalation range is not accessible due to limitations imposed by structural changes or detrimental interaction with the electrolyte at high charging potentials. Li_xFePO₄, on the other hand, can undergo complete lithiation-delithiation cycling without any significant changes in the material's structure, which leads to the impressive stability of the capacity of Li_xFePO₄ cathodes during prolonged cycling.⁴ A major disadvantage of this material is its low intrinsic electrical conductivity.^{1,2,4} However many research groups have presented convincing ways to overcome the intrinsic low electrical conductivity of LiFePO₄, thus demonstrating a fast rate performance of Li_xFePO₄ cathodes in Li-ion battery systems.⁵⁻¹⁰ While all of the above has shown that Li_xFePO₄-based cathodes demonstrate promising electrochemical characteristics at room temperature, there is evidence that at elevated temperatures the olivine undergoes iron dissolution.^{11,12} This is highly important and could be detrimental to its commercialization. Transition metal dissolution under certain conditions (especially at elevated temperatures) is also a critical problem of many Li_xMO_y cathode materials (M = transition metals such as Co, Ni, Mn).¹³⁻¹⁵ Along with capacity fade, this can lead to irreversible changes in the structure of these materials and the formation of inactive phases on the surface of the Li_xMO_y particles, which interfere with the kinetics of Li insertion-deinsertion processes. In addition, the transition metal ions that dissolve from the cathode materials, are reduced on the negative electrodes to metallic clusters, which is well known to affect very badly the passivation of the anodes in Li battery systems.^{12,16} This was demonstrated to be the major source of capacity loss in LiFePO₄/graphite cells at elevated temperature, more so than dissolution of iron from the cathode.¹²

When the graphitic carbon was replaced with an anode which operates at a potential above the reduction to iron metal, only the

cells with the graphite anode experienced significant capacity fading even though some Fe dissolution was reported in both cases at 37 and 55°C.¹² The iron dissolution was connected to the presence of HF in LiPF₆. Indeed, the use of solutions containing lithium bisoxalateborate (LiBOB) resulted in less capacity fading, although some was still observed.¹²

To address the underlying issues related to the stability and capacity fading of LiFePO₄ electrodes, we employed a combination of surface/spectroscopic/electrochemical techniques [voltammetry, impedance spectroscopy, inductively coupled plasma spectroscopy (ICP), X-ray diffraction (XRD), Fourier transform infrared (FTIR) analysis, and photoelectron and Raman spectroscopies] to examine the interfacial chemistry of LiFePO₄ and the conditions for its stabilization as a cathode at elevated temperature. The stability of LiFePO₄ cathodes in terms of iron dissolution was measured at 30 and at 60°C in three types of solutions based on ethylene and dimethyl carbonate mixtures (EC-DMC 1:1): The use of LiClO₄ as the electrolyte enables us to obtain solutions with no acidic contamination. 1 M LiPF₆ solutions can be considered as electrolytes which may contain up to hundred ppms of HF^{17,18} (even when dry). Water contaminated LiPF₆ solutions were also examined as an especially corrosive medium. Of particular interest, we report here that acid scavenger additives in the electrolyte solutions stabilize LiFePO₄ and avoid iron dissolution. The novelty of this work compared to previous studies (e.g., Ref. 11 and 12 mentioned above) lays on the clear correlation between solutions composition (in terms of protic contaminants), iron dissolution, and the electrochemical behavior of LiFePO₄ electrodes at room temperature and at elevated temperatures demonstrated herein and a progress in the understanding of the surface chemistry of these systems by the use of several spectroscopic techniques in conjunction with electrochemical tools in a single study.

Experimental

The LiFePO₄ materials used in this work were prepared by hydrothermal synthesis. The reagents H₃PO₄, (NH₄)₂Fe(SO₄)₆·H₂O, 3LiOH·H₂O, and ascorbic acid (1 wt %) were combined in a 45 mL Parr autoclave in a 1:1:3:0.06: molar ratio and water was added to make up a 67% fill. The autoclave was heated at 205°C for 5 h, cooled to room temperature, and the crystalline solid was separated by filtration and washed with water to remove traces of surfactant or other contaminants. The solid was then ball-milled at 600 rpm for 30 min in a Fritsch Pulverisette using silicon nitride media. The milled mixture was then heated to 600°C for 6 h under an Ar atmosphere. The product was single phase LiFePO₄, as determined by its

* Electrochemical Society Active Member.

^z E-mail: DoronI@mail.biu.ac.il

XRD pattern, containing 1.8% carbon by weight as analyzed by standard gravimetric analysis. The composite electrodes contained LiFePO_4 as the active mass (~80% by weight), carbon black, an additional conductive additive, and a polyvinylidene difluoride (PVDF) binder (~10% each by weight) on Al foil current collectors.

For the spectroscopic measurements, we used electrodes comprising aluminum foil in which LiFePO_4 particles were embedded by pressure. LiFePO_4 powder was pressed onto the foil by a hydraulic press. The exact load of the active mass per cm^2 was measured by weight. Two- and three-electrode coin-type cells were prepared under a highly pure Ar atmosphere in VAC Inc. glove boxes, using standard 2032 cells from NRC Inc. (Canada), in which metallic lithium foils were used as counter and reference electrodes. Detailed preparation of the electrodes is described elsewhere.¹⁹

The electrolyte solutions included 1 M LiClO_4 and 1 M LiPF_6 in EC-DMC 1:1 mixtures, Li battery grade, from Merck Inc. and Tomiyama Inc. and were used as received. We also used LiPF_6 solutions that were deliberately contaminated by 100 ppm of water. Storage and electrochemical measurements were carried out at 30 and 60°C using the appropriate thermostats. Reagents such as Li_2CO_3 , silazane and silazide (LiTMSA) were obtained from Aldrich. The concentration of the additives in solutions was about 1% by weight. The techniques and instrumentation included elemental analysis by ICP, using an Ultima 2, Jobin-Yvon-Horiba spectrometer, a MicroRaman spectrometer from Jovin-Yvon Inc. with an Ar 514.5 nm laser, an FTIR spectrometer from Nicolet Inc. (Magna 860), placed in an H_2O - and CO_2 -free atmosphere in a glove box, in reflectance mode, an XPS system from Kratos, England (the HAXIS model) and standard electrochemical techniques (voltammetry and EIS) using a Solartron Inc. multichannel system, model 1470A and a frequency response analyzer (FRA), model 1255, from the same company. For iron dissolution tests, 50–100 mg of the olivine compound was stored in closed vials containing 1 mL of an electrolyte solution under Ar atmosphere. The solution was removed after a period of storage at 30 or at 60°C and was analyzed by ICP for the presence of iron. Electrodes comprising LiFePO_4 powder on Al foil were treated electrochemically in coin-type cells. The electrodes (containing no additives) were removed from the electrolyte solution, washed several times with highly pure THF, and transferred under pure Ar atmosphere to FTIR, Raman or XPS spectrophotometers. The FTIR measurements were carried out in reflectance mode using a grazing angle attachment (FT80) from Spectratech Inc. The electrodes were sufficiently reflective to provide a valuable spectral response. A nickel mirror was used for the reference spectra. Samples for XPS were transferred from the glove box (highly pure Ar atmosphere) to the high vacuum system of the spectrometer, using a home made transfer system that contains a magnetic manipulator and a gate valve.

Results and Discussion

Figure 1 presents the amount of iron dissolution from LiFePO_4 samples stored at 30 and 60°C in three solutions: 1 M LiClO_4 , 1 M LiPF_6 , and 1 M LiPF_6 + 100 ppm H_2O in EC-DMC 1:1 mixtures. We also stored LiFePO_4 samples in 1 M LiPF_6 solutions containing 1 wt % Li_2CO_3 , 1,3-diphenyl-1,1,3,3-tetramethyl disilazane and Libis (Trimethylsilyl)amide (LiTMSA). As seen, in a 1 M LiClO_4 solution LiFePO_4 does not dissolve even at 60°C after weeks of storage. In a LiPF_6 solution that may contain up to hundred ppm of HF, the amount of iron dissolution from LiFePO_4 during 30 days of storage was 3–4% at 30°C and about 20% at 60°C. The highest level of iron dissolution was measured in the H_2O -contaminated solution, 5–6% at 30°C and up to 60% at 60°C. The presence of silazane, silazide (see their structural formulae in Fig. 1), or Li_2CO_3 in the solutions containing acidic and protic contaminants, considerably reduces iron dissolution in these systems, as also indicated in Fig. 1.

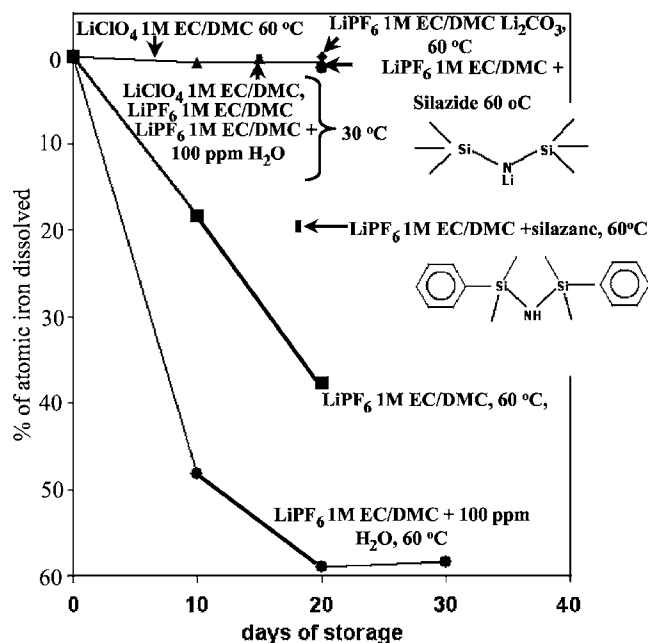
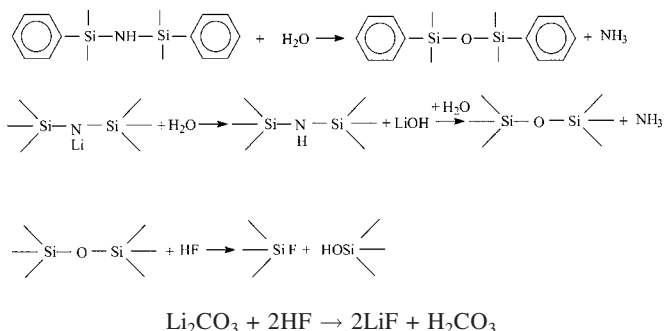


Figure 1. Results of iron dissolution tests (measured by ICP). LiFePO_4 samples (50–100 mg) were stored in 1 M LiClO_4 , 1 M LiPF_6 , and 1 M LiPF_6 + 100 ppm H_2O solutions in EC-DMC 1:1 (1 mL) at 30 and 60°C, as indicated. The effect of acid scavenger additives, Li_2CO_3 , silazane, and silazide compounds, 1 wt% (the structural formulae appear in the figure) was also measured, as indicated.

The reactions of these three reagents with H_2O and HF are shown below



(weak acid).

These results indicate that in dry solutions containing no acidic contaminants, LiFePO_4 is highly stable, even at elevated temperatures.

Iron dissolution is probably caused by the presence of H_3O^+ ions in solutions that can react with the olivine and lead to ion exchange ($2\text{H}^+ \leftrightarrow \text{Fe}^{2+}$), as can be concluded from previous studies.^{11,12} The ratio between the mass of solution and the LiFePO_4 in our experiments (10:1) is much higher by more than one order of magnitude compared to the in practical battery systems. However, in the latter, the transition metal ions dissolved from the cathodes, are reduced on the negative electrode. Thereby, even if quick saturation of the dissolved transition metal ions in the electrolyte solution can be reached in practical batteries due to the small amount of solution used, the transition metal ions are continuously removed from the solutions due to their reaction on the anode side. This is highly detrimental to the passivation of the anode as explained previously.^{12,16} Consequently, despite the fact that the electrolyte/olivine ratio in the tests described herein is much higher compared to practical systems, the results presented in Fig. 1 are significant. They demonstrate critical conditions for enhanced detrimental pro-

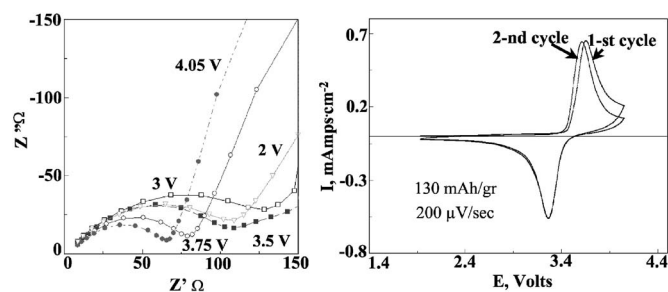


Figure 2. Typical first and second CVs and impedance spectra (Nyquist plots) measured at several potentials, with composite LiFePO_4 electrodes in LiClO_4 solutions at 30°C . The electrode's capacity potential, scan rate (CV), and the potential in which impedance spectra were measured (at equilibrium) are indicated in the figure.

cesses connected to iron dissolution and the possibility of attenuating this phenomenon by the use of acid scavengers in solutions. The reaction of LiFePO_4 in corrosive media, (i.e., 60°C in LiPF_6 solutions) also implies that there should be bulk changes in the active mass, that we attempted to quantify using XRD as reported elsewhere.²⁰ The patterns included mostly LiFePO_4 peaks of lower intensity than those of the pristine samples. Hence, we conclude that the bulk changes that accompany iron dissolution from LiFePO_4 upon aging, may form amorphous phases.

As a reference, Fig. 2 presents the typical electrochemical behavior of composite LiFePO_4 electrodes in uncontaminated solutions, e.g., 1 M LiClO_4 EC-DMC, including slow scan rate CV and impedance spectra at several equilibrium potentials. Usually, composite electrodes comprising LiCoO_2 , LiNiO_2 , or LiMn_2O_4 reach steady state behavior only after a few initial cycles, during which their capacity changes (usually increases from an initial lower value). With all the composite LiFePO_4 electrodes tested in LiClO_4 solutions, the steady state capacity was reached in the first cycle (this could approach the theoretical value at certain conditions, depending on scanning rates and temperature). Figure 2 shows typical first and second consecutive CVs of such a system. The fact that the first and second anodic peaks do not overlap may relate to the improvement in the impregnation of the solution into the composite (porous) elec-

trode from the first to the second anodic polarization and also due to fractures in the carbon coating that occur during the first delithiation of the material.

The impedance spectra of these electrodes presented as Nyquist plots includes two main features: a flat semicircle related to the high-medium frequencies and a steep Z'' vs Z' line, related to the low frequencies. The application and interpretation of these spectra is not trivial. When a red-ox reaction occurs via a first order phase transition, it means that the electrochemical process is not fully reversible. However, that is a condition for the validity of the impedance spectral response to the low amplitude alternating voltage used to stimulate the electrode in EIS measurements. The hysteresis in an electrochemical reaction involving a phase transition, as reflected by the peak separation (see the CVs in Fig. 2), may be too pronounced for the reliable application of impedance spectroscopy. Diffusion coefficient calculations by Prossini et al.²¹ show that the kinetics related to the phase transition of LiFePO_4 is even slower compared to lithiated transition metal oxides such as LiNiO_2 .²²

Nevertheless, impedance spectroscopy should be meaningful at the high-frequency domain, which reflects the fast processes: interfacial charge transfer, which includes Li-ion transfer across the solution/host interface, and the migration of Li-ions through surface films, coupled with the relevant capacitances (e.g., surface films and double layer capacitances). Because the phase transition is supposed to be slower than the interfacial processes, its impedance response may be similar to that of ideally polarized electrodes. A general property of the impedance response of LiFePO_4 electrodes, as demonstrated in Fig. 2, is that upon deintercalation, as the potential is higher, the high-frequency impedance is lower. This is reflected by the contraction of the semicircle in the relevant Nyquist plots.

Figure 3 compares initial CVs and impedance spectra of Li_xFePO_4 electrodes measured after stabilization by two delithiation-lithiation cycles, with those of the same electrodes after aging. Electrodes aged in LiPF_6 solutions at 30°C retain their capacity and their impedance decreases. This may be caused by the impregnation of the entire active mass with solution. The behavior correlates with the stability of LiFePO_4 in standard LiPF_6 solutions at 30°C (see Fig. 1). However, at 60°C , the voltammetric behavior of the LiFePO_4 cathodes in LiPF_6 solutions reflects very sluggish kinetics and an increase in the electrode's impedance upon storage (see the middle charts in Fig. 3 and the broad CV peaks measured with Li_xFePO_4 electrodes at 60°C). The above features correlate

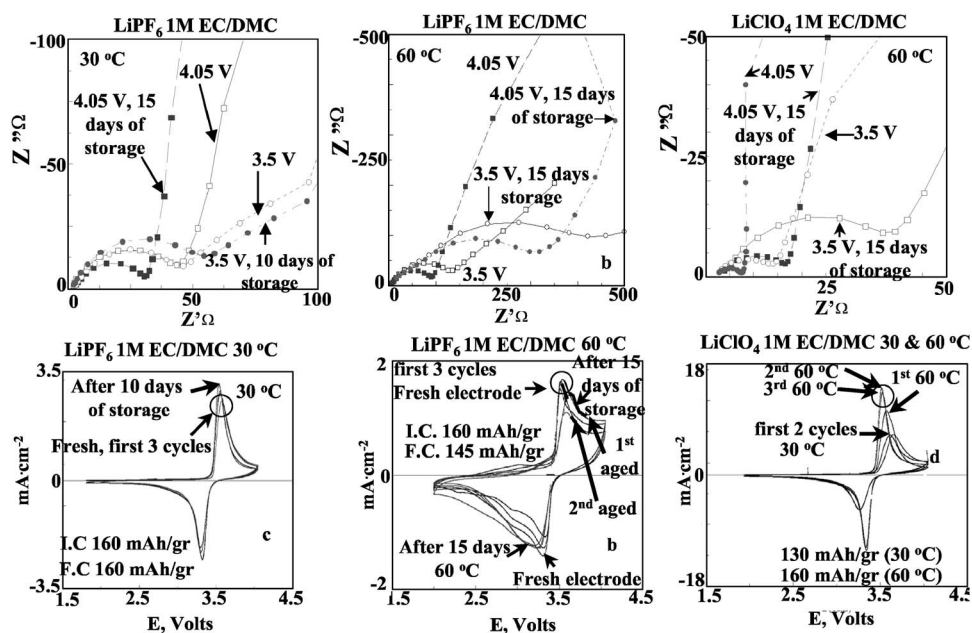


Figure 3. A comparison between pristine and aged LiFePO_4 electrodes stored at 30°C and 60°C in LiPF_6 and LiClO_4 solutions using CV and EIS (Nyquist plots), as indicated. The solution, temperature, initial and final capacities (I.C., F.C), and equilibrium potentials in which the impedance spectra were measured, are marked on the charts. The scan rate for the CV measurements was $200 \mu\text{V/s}$. 1st, 2nd etc. marked in the charts, relate to the consecutive CV cycles.

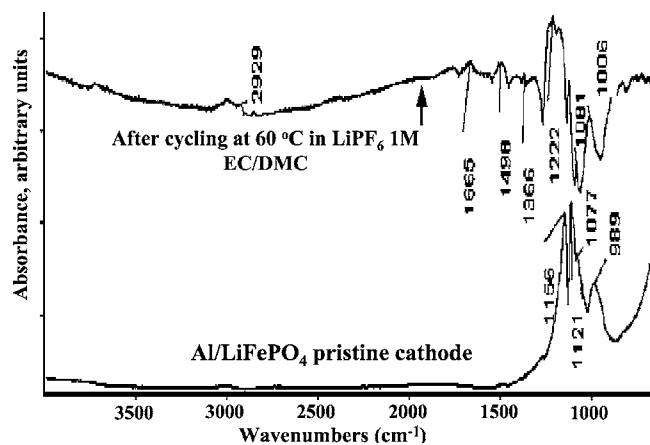


Figure 4. FTIR spectra measured ex situ in reflectance mode from pristine and cycled (1 M LiPF₆ EC-DMC solution, 60°C) LiFePO₄ electrodes (indicated). Some peak frequencies are marked on the chart. The electrodes comprised LiFePO₄ powder embedded in Al foil (no binder or carbon additives).

with the pronounced dissolution of iron under these conditions. The behavior of the LiFePO₄ electrodes in LiClO₄ solutions (i.e., no acidic contaminants, dry solutions) is presented in the right hand charts in Fig. 3. The electrode's kinetics at 60°C is fast, as reflected by the electrochemical response. A capacity close to the theoretical one can be obtained. Although the electrode's impedance increases upon storage, it is much lower compared to that developed in the LiPF₆ solutions as seen by comparing the middle and upper right charts in Fig. 3. Hence, it is clear that the poor behavior of Li_xFePO₄ electrodes at elevated temperatures in LiPF₆ solutions is connected to the presence of acidic contamination, which in turn leads to iron dissolution as previously suggested.^{11,12}

Figure 4 shows FTIR spectra of a pristine Al/LiFePO₄ electrode and a similar electrode after cycling in a 1 M LiPF₆ solution at 60°C. The changes between the two spectra are spectacular. The spectrum of the pristine and cycled electrodes shows several pronounced IR peaks around 1200–1000 cm⁻¹, which can be attributed to P–O bond vibrations.²³ However, the spectrum from the cycled electrode also displays new peaks in the 3000–2900 cm⁻¹ (C–H

stretching vibrations), 1700–1300, 1250–1100, and 900–700 cm⁻¹ regions. These spectra are not conclusive enough to enable the unambiguous identification of the new products. However, it is clear that the electrodes develop rich surface chemistry in LiPF₆ solutions at elevated temperatures. The species thus formed include organic compounds that result from the decomposition of solvent molecules and include C–H and C=O bonds (peaks around 3000–2900 and 1700–1600 cm⁻¹, respectively)²⁴. New peaks in the 1250–1100 cm⁻¹ region may reflect C–O bonds,²⁴ and the peaks in the 900–800 cm⁻¹ region may reflect P–F bonds.²⁵

Complementary information was obtained from XPS measurements. Figure 5 shows the F 1s, C 1s, O 1s, and P 2s spectra of pristine and aged electrodes (60°C, LiPF₆ solution). The F 1s spectra demonstrate the formation of surface LiF from the presence of the peak at 685–686 eV. Other fluorine compounds with a higher oxidation state of the fluorine atoms (another peak at 689–687 eV), may reflect the formation of surface Li_xPF_y or Li_xPO_yF_z species, which correlate with the IR peaks around 900–800 cm⁻¹. As expected, the oxygen spectra show very slight changes. The P 2s spectra of aged electrodes have a lower intensity than the pristine and there is a shift of the broad P 2s peak to higher eV values. These changes can be explained by the coverage of the active mass by surface species, arising from reactions of solution species and the formation of new surface compounds with P–F bonds. The C 1s spectra of aged electrodes also reflect the formation of organic surface species that contain C–O and C=O bonds (peaks around 287 and 290 eV). Thus, both XPS and IR measurements are consistent in demonstrating reactions of the active mass, which occur with solution species at elevated temperatures. Inorganic surface species such as LiF, Li_xPF_y, and Li_xPO_yF_z, as well as organic, carbonyl-containing surface species are formed. This in turn explains the high impedance of Li_xFePO₄ electrodes, which is developed in LiPF₆ solutions, as LiF films, which are always formed in them, are highly resistive to Li-ion migration.²⁶

Figure 6 compares Raman spectra of a pristine electrode with that of electrodes aged in different solutions. Because Raman spectroscopy relates mostly to the bulk the intrinsic LiFePO₄ peaks (marked in the spectra of Fig. 6) appear in all the spectra of the aged electrodes. The most pronounced peaks around 1359 and 1600 cm⁻¹ are related to the amorphous carbon,²⁷ which is intrinsically part of the active mass due to the synthesis conditions. The presence of this

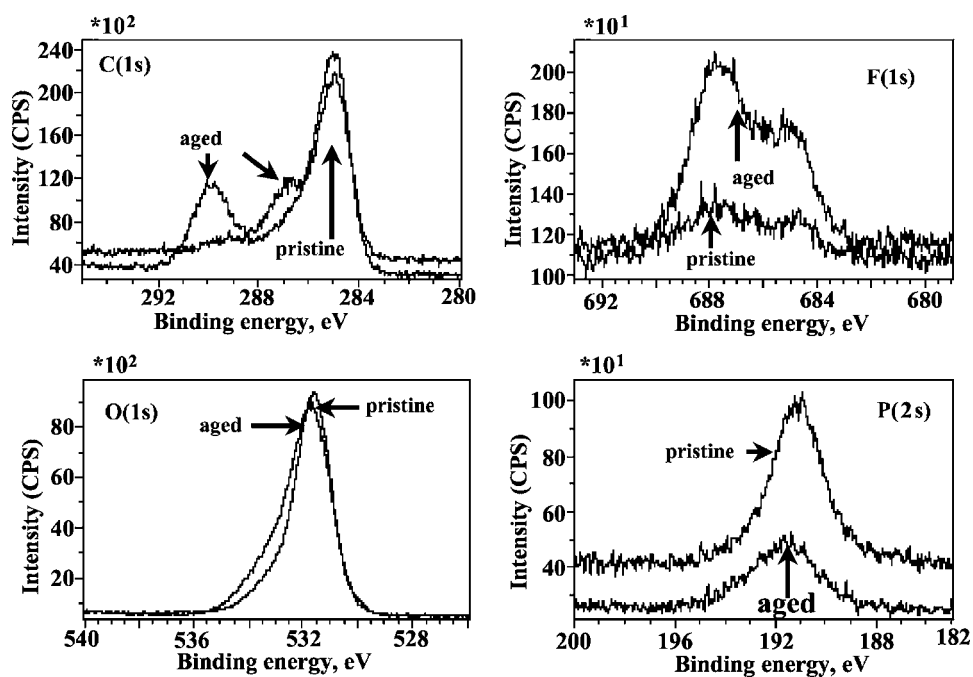


Figure 5. XPS data, including typical F 1s, C 1s, O 1s, and P 2s spectra of pristine and aged LiFePO₄ electrodes (1 M LiPF₆ EC-DMC solution, 60°C), as marked on the charts. The electrode comprised LiFePO₄ powder embedded in Al foil (no binder and carbon additives).

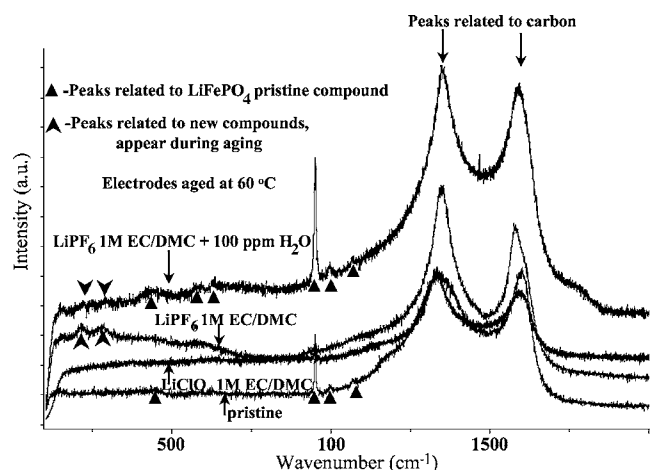


Figure 6. Raman spectra measured from pristine and aged electrodes. The relevant solutions in which the electrodes were aged are marked near the spectra. Peaks related to LiFePO_4 and to new products (due to aging) are marked. The electrodes comprised LiFePO_4 powder embedded in Al foil (no binder and carbon additives).

carbon leads to the sufficient electronic conductivity of the active mass, and in fact enables the operation of these electrodes at high capacity and rates. It is clear that electrodes aged in LiClO_4 solutions have nearly the same Raman spectra as those of the pristine electrodes in accord with the stability seen in LiClO_4 solutions (Fig. 1-3). The Raman spectra of electrodes aged at 60°C in the corrosive solutions (LiPF_6 , dry and wet), however, shows new peaks. Although these features are weak and not diagnostic of the new phases that are formed, they indicate clearly the bulk changes of the active mass.

Conclusion

LiFePO_4 electrodes are stable in standard LiPF_6 solutions at ambient temperature. This is reflected by the negligible iron dissolution upon storage, stable electrochemical response, and by the fact that the electrode's impedance does not increase during prolonged storage in solutions. It can be said that LiFePO_4 electrodes are more stable and less reactive in standard (LiPF_6) solutions at ambient temperatures than many other types of cathodes, such as LiCoO_2 , LiNiO_2 , LiMn_2O_4 , and derivatives of these materials (e.g., $\text{LiNi}_{1-x}\text{M}_x\text{O}_2$ or $\text{LiMn}_{2-x}\text{M}_x\text{O}_4$, M = other transition metal). However, at elevated temperatures, LiPF_6 solutions, especially wet ones, are corrosive to LiFePO_4 .

Aging of Li_xFePO_4 cathodes in LiPF_6 solutions at 60°C leads to capacity fading, which relates to iron dissolution and a pronounced increase in the electrodes impedance, and the kinetics become very sluggish. EIS, FTIR, and XPS, and Raman spectroscopy (to some

extent), showed that LiFePO_4 electrodes develop resistive surface films that include LiF , phosphorous compounds with P-F or O-P-F bonds, and organic surface species. However, it was impossible to identify the exact composition of the surface films and the bulk phases that are formed on the Li olivine compounds upon aging in solutions. The detrimental effect of acidic contamination in solutions on the stability of LiFePO_4 cathodes is obvious, and hence can be largely avoided by using solutions containing no acidic contaminants. This can be achieved by the choice of the appropriate salt, (e.g., the replacement of LiPF_6 by LiClO_4). However, because the replacement of the standard LiPF_6 salt by any other alternative electrolyte is not yet realistic, iron dissolution in LiPF_6 solutions at elevated temperatures can be minimized by the use of acid scavenger additives such as organosilicon and/or basic compounds.

Bar-Ilan University assisted in meeting the publication costs of this article.

References

1. A. K. Padhi, K. S. Nanjundaswamy, and J. B. Goodenough, *J. Electrochem. Soc.*, **144**, 1188 (1997).
2. D. K. Kim and J. Kim, *Electrochem. Solid-State Lett.*, **9**, A439 (2006).
3. T. Ohzuku, A. Ueda, M. Nagayama, Y. Iwakoshi, and H. Komori, *Electrochim. Acta*, **38**, 1159 (1993).
4. K. Striebel, J. Shim, A. Sierra, H. Yang, X. Y. Song, R. Kostecki, and K. McCarthy, *J. Power Sources*, **146**, 33 (2005).
5. N. Ravet, Y. Chouinard, J. F. Magnan, S. Besner, M. Gauthier, and M. Armand, *J. Power Sources*, **97-8**, 503 (2001).
6. H. Huang, S. C. Yin, and L. F. Nazar, *Electrochem. Solid-State Lett.*, **4**, A170 (2001).
7. S. Y. Chung, J. T. Bloking, and Y. M. Chiang, *Nat. Mater.*, **1**, 123 (2002).
8. P. S. Herle, B. Ellis, N. Coombs, and L. F. Nazar, *Nat. Mater.*, **3**, 147 (2004).
9. T. Nakamura, Y. Miwa, M. Tabuchi, and Y. Yamada, *J. Electrochem. Soc.*, **153**, A1108 (2006).
10. J. Molenda, *Materials Science-Poland*, **24**, 61 (2006).
11. N. Iltchev, Y. K. Chen, S. Okada, and J. Yamaki, *J. Power Sources*, **119**, 749 (2003).
12. K. Amine, J. Liu, and I. Belharouak, *Electrochem. Commun.*, **7**, 669 (2005).
13. W. Choi and A. Manthiram, *J. Electrochem. Soc.*, **153**, A1760 (2006).
14. H. W. Chan, J. G. Duh, and S. R. Sheen, *Electrochim. Acta*, **51**, 3645 (2006).
15. Y. Iriyama, K. Nishimoto, C. Yada, T. Abe, Z. Ogumi, and K. Kikuchi, *J. Electrochem. Soc.*, **153**, A821 (2006).
16. G. G. Amatucci, J. M. Tarascon, and J. C. Klein, *Solid State Ionics*, **83**, 167 (1996).
17. R. Oesten, U. Heider, and M. Schmidt, *Solid State Ionics*, **148**, 391 (2002).
18. T. Kawamura, S. Okada, and J. Yamaki, *J. Power Sources*, **156**, 547 (2006).
19. D. Aurbach, B. Markovsky, A. Rodkin, E. Levi, Y. S. Cohen, H.-J. Kim, and M. Shmidt, *Electrochim. Acta*, **47**, 4291 (2002).
20. M. Koltypin, B. Ellis, L. F. Nazar, and D. Aurbach, *J. Power Sources*, Submitted.
21. P. P. Prosini, M. Lisi, D. Zane, and M. Pasquali, *Solid State Ionics*, **48**, 45 (2002).
22. M. D. Levi, K. Gamolsky, U. Heider, R. Oesten, and D. Aurbach, *J. Electroanal. Chem.*, **477**, 32 (1999).
23. X. H. Guan, C. Shang, J. Zhu, and G. H. Chen, *J. Colloid Interface Sci.*, **293**, 296 (2006).
24. R. M. Silverstein, C. G. Bassler, and T. C. Morrill, in *Spectroscopic Identification of Organic Compounds*, p. 73, John Wiley & Sons, New York (1974).
25. D. Aurbach, M. Moshkovich, Y. Cohen, and A. Schechter, *Langmuir*, **15**, 2947 (1999).
26. D. Aurbach, K. Gamolsky, B. Markovsky, G. Salitra, and Y. Gofer, *J. Electrochem. Soc.*, **147**, 1322 (2000).
27. J. T. Chen, K. Shin, J. M. Leiston-Belanger, M. F. Zhang, and T. P. Russell, *Adv. Funct. Mater.*, **16**, 1476 (2006).